4th International Conference on
Earthquake Geotechnical Engineering
June 25-28, 2007
Paper No. 1249

DETERMINATION OF POINT OF APPLICATION OF SEISMIC ACTIVE THRUST ON RETAINING WALL

Deepankar CHOUDHURY [1], Sanjay NIMBALKAR[2]

ABSTRACT

Design of retaining wall needs the complete knowledge of active earth pressure. Under earthquake condition, the design requires special attention to reduce the devastating effect of this natural hazard. But under seismic condition, most of the available literatures starting from the pioneering work of Mononobe-Okabe (1926, 1929) [see Kramer, 1996] to the latest work of Choudhury and Singh (2006) give the pseudo-static analytical values of the active earth pressures as an approximate solution to the real dynamic nature of the complex problem. In this pseudo-static method, only the magnitudes of the peak ground accelerations at a particular instant of time are assumed to act with the inertia component of the soil mass along with other static forces. Hence, the total active thrust obtained by this analysis is analogous to the static active thrust analysis with different magnitudes, and the variation of earth pressure along the height of the retaining wall remains linear though the computation of correct point of application of total seismic active thrust is important for the design purpose of the wall. But there is no scope to find out the point of application of seismic active thrust by pseudo-static approach but to assume it to act at one-third height from the base of the wall. Moreover, in this pseudo-static method, neither the time dependent effect of applied earthquake load nor the effect of shear and primary waves passing through the soil media are considered. Correcting these errors, in recently developed pseudo-dynamic method of analysis, all these variations are considered to compute seismic active earth pressures [Steedman and Zeng, 1990; Choudhury *et al.*, 2006; Choudhury and Nimbalkar, 2006]. But the complete solution to compute the point of application of seismic active thrust which is very impotant for design of the wall is still scarce. In this paper, a complete closed-form solution for computing the point of application of seismic active thrust using limit equilibrium method of analysis with pseudo-dynamic approach is adopted. In the present work the effect of variation of parameters like soil friction angle, wall friction angle, time period of earthquake ground motion, seismic shear and primary wave velocities of backfill soil, soil amplification and seismic peak horizontal and vertical ground accelerations on the seismic active earth pressure are studied. As expected, the present results show that with seismicity, the point of application of seismic active thrust varies a lot, compared to a constant value mentioned in pseudo-static method of analysis. It is found that the point of application of seismic active thrust is above one-third from the base of the wall compared to the static value of one-third from the base of the wall. Also this location shifts away from the base of the wall with increase in interfacial soil-wall friction. It is also found that the present results give higher design values of the seismic active earth pressure coefficients compared to the conventional pseuso-static Mononobe-Okabe values. The non-linearity of the seismic active earth pressure distribution increases with seismicity compared to a linear pseudo-static seismic active earth pressure distribution. Also the present results obtained by closed-form solution are compared and found to match well with a very few available dynamic centrifuge test results [Steedman and Zeng, 1991] in literature.

Keywords: pseudo-dynamic, soil-wall interface, body waves, amplification, time period

---

[1] Assistant Professor, Department of Civil Engineering, Indian Institute of Technology Bombay, Powai, Mumbai-400 076, INDIA. Email: dc@civil.iitb.ac.in

[2] Research Scholar, Department of Civil Engineering, Indian Institute of Technology Bombay, Mumbai, INDIA.

INTRODUCTION

Evaluation of seismic active earth pressure is essential for the safe design of rigid retaining wall in the seismic zone. In the past, many researchers have developed several methods to determine the seismic active earth pressure on a rigid retaining wall. The pioneering work on earthquake-induced lateral active earth pressures acting on a retaining wall were reported by Okabe, 1926 and Mononobe and Matsuo, 1929. This pseudo-static approach following the Coulomb's static earth pressure analysis is known as Mononobe-Okabe method (see Kramer, 1996) to compute seismic earth pressure. Recent works of Richards et al. 1999, Saran and Gupta, 2003, Choudhury and Singh, 2006 and few others also considered the pseudo-static method to compute seismic active earth pressure behind a retaining wall. Green and Ebeling, 2002, 2003, Green et al., 2003 had performed numerical analysis using by using geotechnical software FLAC. However regarding the distribution of dynamic active earth pressure with depth, many authors have commented favorably on the magnitude of the Mononobe-Okabe lateral earth force but have disagreed on the point of application, which indicates the uncertainty over the distribution of seismic active earth pressure with depth. There is no justification in the extended Coulomb's approach adopted by Mononobe-Okabe for the seismic case by assuming the linear active earth pressure distribution with depth. To overcome this drawback, the time and phase difference due to finite shear wave propagation behind a retaining wall was considered using a simple and more realistic way of pseudo-dynamic method, proposed by Steedman and Zeng, 1990. Again Steedman and Zeng, 1991 compared the theoretical results with the centrifuge model test results to validate the pseudo-dynamic method.

Steedman and Zeng, 1990 considered in their analysis a vertical rigid retaining wall supporting horizontal backfill for a particular value of soil friction angle (ϕ) and a particular value of seismic horizontal acceleration ($k_h g$, where g is the acceleration due to gravity) only. But the effect of various parameters such as wall friction angle (δ), soil friction angle (ϕ), time period of earthquake ground motion, seismic shear and primary wave velocities of backfill soil (V_s and V_p), soil amplification factor (f) and seismic peak horizontal and vertical ground accelerations ($k_h g$ and $k_v g$) on the seismic active earth pressure behind a rigid retaining wall by the pseudo-dynamic method didn't get any attention till today. Hence in this paper, a complete closed-form solution for computing the point of application of seismic active thrust using limit equilibrium method of analysis with pseudo-dynamic approach is adopted.

METHOD OF ANALYSIS

Similar to the pseudo-dynamic approach which considers finite shear wave velocity within the backfill material as proposed by Steedman and Zeng, 1990, here also it is assumed that the shear modulus (G) is constant with the depth of retaining wall throughout the backfill.

Consider the fixed base vertical rigid retaining wall AB of height H as shown in Figure 1. The wall is supporting a cohesionless backfill material with horizontal ground. In the present study, both the shear wave velocity, $V_s = (G/\rho)^{1/2}$, where, ρ is the density of the backfill material and primary wave velocity, $V_p = (G(2-2\nu)/\rho(1-2\nu))^{1/2}$, where ν is the poisson's ratio of the backfill are assumed to act within the soil media due to earthquake loading. In the present analysis, the superposition of the shear and primary waves is unlikely because the soil media is considered as a homogeneous, semi-infinite layer instead of a bounded layer. Hence for such an unbounded homogeneous soil layer, it is unlikely to form the standing wave from the superposition of the shear and primary waves in such continuous media (Kramer, 1996). For most geological materials, $V_p/V_s = 1.87$ (Das, 1993). The period of lateral shaking, $T = 2\pi/\omega$ (Kramer, 1996), where ω is the angular frequency is considered in the analysis. A planer rupture surface inclined at an angle, α with the horizontal is considered in the analysis.

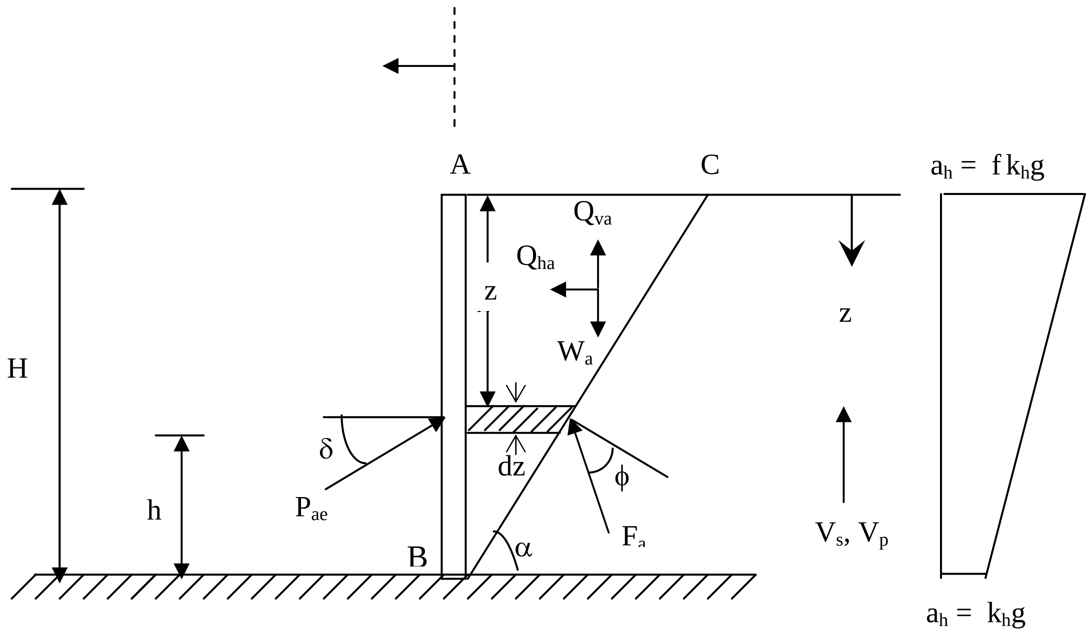

Figure 1. Model retaining wall considered for computation of seismic active earth pressure.

Both the body waves (i.e. shear and primary waves) propagating through the backfill soil are considered to be influenced by the soil amplification and act within the backfill soil due to the earthquake loading. The base of the wall is assumed to be subjected to the harmonic horizontal seismic acceleration with amplitude a_h (= $k_h g$, where g is the acceleration due to gravity) and the harmonic vertical seismic acceleration with amplitude a_v (= $k_v g$). The exact nature of the soil amplification is dependent on several factors, such as, the geometry and rigidity of the adjacent structure, the stiffness and damping of the soil, the depth of the soil layer and so on. Again, similar to the assumption made by Steedman and Zeng, 1990, here also the linear variation of the horizontal and vertical seismic accelerations from the input accelerations at the base to the higher value (depending upon the soil amplification) at the top of the retaining wall, such that $k_{h(z = H)} = f\, k_{h(z = 0)}$ and $k_{v(z = H)} = f\, k_{v(z = 0)}$, where f is a constant and is termed as amplification factor, is considered. To obtain the critical design value of the seismic earth pressures, it is assumed that both the horizontal and vertical vibrations start at exactly the same time without any phase shift between these two vibrations, which is the worst possible combination of earthquake loading. Referring to Figure 1, the horizontal and the vertical acceleration at any depth z and time t, below the top of the wall can be expressed as,

$$a_h(z,t) = \left\{1 + \frac{H-z}{H}(f-1)\right\} k_h.g.\sin w\left(t - \frac{(H-z)}{V_s}\right) \tag{1}$$

$$a_v(z,t) = \left\{1 + \frac{H-z}{H}(f-1)\right\} k_v.g.\sin w\left(t - \frac{(H-z)}{V_p}\right) \tag{2}$$

The mass of a thin element of the wedge at depth z (Figure 1) is,

$$m(z) \;=\; \frac{\gamma}{\text{g}} \frac{H-z}{\tan\alpha} dz \tag{3}$$

where, γ is the unit weight of the backfill.

The total horizontal inertia force acting within the failure zone can be expressed as,

$$Q_h(t) = \int_0^H m(z) a_h(z, t) dz \tag{4}$$

$$Q_h(t) = \frac{TV_s \ \gamma \ k_h}{4\pi^2 \tan\alpha}\left[2\pi H \cos w\zeta + TV_s(\sin w\zeta - \sin wt)\right] + \frac{TV_s \ \gamma \ k_h\left(f_a - 1\right)}{4\pi^3 H \tan\alpha}\left[2\pi H\left(\pi H \cos w\zeta + TV_s \sin w\zeta\right) + \left(TV_s\right)^2(\cos wt - \cos w\zeta)\right] \tag{5}$$

where, $\lambda = TV_s$ is the wavelength of the vertically propagating shear wave and $\zeta = t - H/V_s$.

Now, the total vertical inertia force acting within the failure zone can be expressed as,

$$Q_v(t) = \int_0^H m(z) a_v(z, t) dz \tag{6}$$

$$Q_v(t) = \frac{TV_p \ \gamma \ k_v}{4\pi^2 \tan\alpha}\left[2\pi H \cos\omega\psi + TV_p(\sin\omega\psi - \sin\omega t)\right] + \frac{TV_p \gamma k_v\left(f - 1\right)}{4\pi^3 H \tan\alpha}\left[2\pi H\left(\pi H \cos\omega\psi + TV_p \sin\omega\psi\right) + \left(TV_p\right)^2(\cos\omega t - \cos w\psi)\right] \tag{7}$$

where, $\eta = TV_p$, is the wavelength of the vertically propagating primary wave and $\psi = t - H/V_p$.

Though the horizontal acceleration is acting from left to right and vice-versa and the vertical acceleration is acting from top to bottom and vice-versa, only the critical combination of directions of $Q_h(t)$ and $Q_v(t)$ are considered, which give the maximum seismic active earth pressure for the design of the wall.

The special case of a rigid wedge is given, in the limit as

$$\lim_{v_s \to \infty}(Q_h)_{\max} = \frac{\gamma H^2 a_h}{2g\tan\alpha} = \frac{a_h}{g}W = k_h W \tag{8}$$

$$\lim_{v_P \to \infty}(Q_v)_{\max} = \frac{\gamma H^2 a_v}{2g\tan\alpha} = \frac{a_v}{g}W = k_v W \tag{9}$$

which is equivalent to the pseudo static force assumed in the Mononobe-Okabe method.

The total (static and seismic) active thrust, $P_{ae}(t)$ can be obtained by resolving the forces on the wedge as shown in Figure 1) and considering the equilibrium of the forces. Hence $P_{ae}(t)$ can be expressed as follows,

$$P_{ae}(t) = \frac{W\sin(\alpha - \phi) + Q_h(t)\cos(\alpha - \phi) + Q_v(t)\sin(\alpha - \phi)}{\cos(\delta + \phi - \alpha)} \tag{10}$$

where, W is the weight of the failure zone, ϕ is the soil friction angle and δ is the wall friction angle.

The seismic active earth pressure coefficient, K_{ae} is defined as,

$$K_{ae} = \frac{2P_{ae}}{\gamma H^2} \tag{11}$$

Substituting for $Q_h(t)$ and $Q_v(t)$ in the equation (8), an expression for K_{ae} in terms of $Q_h(t)$, $Q_v(t)$ and W can be derived as,

$$\left.\begin{aligned} K_{ae} = {} & \frac{1}{\tan\alpha}\frac{\sin(\alpha-\phi)}{\cos(\delta+\phi-\alpha)} + \frac{k_h}{2\pi^2\tan\alpha}\left(\frac{TV_s}{H}\right)\times\frac{\cos(\alpha-\phi)}{\cos(\delta+\phi-\alpha)}\times m_1 + \frac{k_v}{2\pi^2\tan\alpha}\left(\frac{TV_p}{H}\right)\times\frac{\sin(\alpha-\phi)}{\cos(\delta+\phi-\alpha)}\times m_2 \\ & + \frac{k_h(f-1)}{2\pi^3\tan\alpha}\left(\frac{TV_s}{H}\right)\times\frac{\cos(\alpha-\phi)}{\cos(\delta+\phi-\alpha)}\times m_3 + \frac{k_v(f-1)}{2\pi^3\tan\alpha}\left(\frac{TV_p}{H}\right)\times\frac{\sin(\alpha-\phi)}{\cos(\delta+\phi-\alpha)}\times m_4 \end{aligned}\right\} \tag{12}$$

where,

$$m_1 = \left[2\pi\cos 2\pi\left(\frac{t}{T}-\frac{H}{TV_s}\right)+\left(\frac{TV_s}{H}\right)\left(\sin 2\pi\left(\frac{t}{T}-\frac{H}{TV_s}\right)-\sin 2\pi\left(\frac{t}{T}\right)\right)\right]$$

$$m_2 = \left[2\pi\cos 2\pi\left(\frac{t}{T}-\frac{H}{TV_p}\right)+\left(\frac{TV_p}{H}\right)\left(\sin 2\pi\left(\frac{t}{T}-\frac{H}{TV_p}\right)-\sin 2\pi\left(\frac{t}{T}\right)\right)\right]$$

$$m_3 = \left[2\pi\left(\pi\cos 2\pi\left(\frac{t}{T}-\frac{H}{TV_s}\right)+\left(\frac{TV_s}{H}\right)\sin 2\pi\left(\frac{t}{T}-\frac{H}{TV_s}\right)\right)+\left(\frac{TV_s}{H}\right)^2\left(\cos 2\pi\left(\frac{t}{T}\right)-\cos 2\pi\left(\frac{t}{T}-\frac{H}{TV_s}\right)\right)\right]$$

$$m_4 = \left[2\pi\left(\pi\cos 2\pi\left(\frac{t}{T}-\frac{H}{TV_p}\right)+\left(\frac{TV_p}{H}\right)\sin 2\pi\left(\frac{t}{T}-\frac{H}{TV_p}\right)\right)+\left(\frac{TV_p}{H}\right)^2\left(\cos 2\pi\left(\frac{t}{T}\right)-\cos 2\pi\left(\frac{t}{T}-\frac{H}{TV_p}\right)\right)\right]$$

From equation (12), it is seen that K_{ae} is function of the dimensionless parameters H/TV_s, H/TV_p, t/T, f and the wedge angle α.

The maximum value of K_{ae} is obtained by optimizing K_{ae} with respect to t/T and α. It is found that K_{ae} is a function of H/TV_s, H/TV_p, which is the ratio of time for a shear wave and primary wave to travel the full height of the wall to the period of lateral shaking and amplification factor f. Using excel spreadsheet tool 'SOLVER', optimization of K_{ae} is done.

Total seismic active thrust can also be defined as,

$$P_{ae} = P_{as} + P_{ahd} + P_{avd} \tag{13}$$

where, P_{as} is the pressure acting on the retaining wall due to vertical weight of the wedge,
P_{ahd} is the pressure acting on the wall due to horizontal inertia of the wedge and
P_{avd} is the pressure acting on the wall due to vertical inertia of the wedge.

And the seismic active earth pressure distribution can be obtained by differentiating the total active thrust with respect to the depth of the wall as given by,

$$p_{ae}(t) = \frac{\partial P_{ae}(t)}{\partial z} \tag{14}$$

$$\left.\begin{aligned} p_{ae}(t) &= \frac{k_h \gamma z}{\tan\alpha} f \frac{\cos(\alpha-\phi)}{\cos(\delta+\phi-\alpha)} \sin\left[w\left(t-\frac{z}{V_s}\right)\right] + \left(\frac{\gamma\, z}{\tan\alpha} + \frac{k_v \gamma z}{\tan\alpha} f \sin\left[w\left(t-\frac{z}{V_p}\right)\right]\right) \frac{\sin(\alpha-\phi)}{\cos(\delta+\phi-\alpha)} \\ &+ \frac{k_h \gamma}{\tan\alpha}(f-1)\frac{\cos(\alpha-\phi)}{\cos(\delta+\phi-\alpha)} \frac{TV_s}{2\pi}\left[-\cos w\left(t-\frac{z}{V_s}\right) - \frac{TV_s}{\pi z}\sin w\left(t-\frac{z}{V_s}\right) + \frac{(TV_s)^2}{2\pi^2 z^2}\left(\cos w\left(t-\frac{z}{V_s}\right) - \cos wt\right)\right] \\ &+ \frac{k_v \gamma}{\tan\alpha}(f-1)\frac{\sin(\alpha-\phi)}{\cos(\delta+\phi-\alpha)} \frac{TV_p}{2\pi}\left[-\cos w\left(t-\frac{z}{V_p}\right) - \frac{TV_p}{\pi z}\sin w\left(t-\frac{z}{V_p}\right) + \frac{(TV_p)^2}{2\pi^2 z^2}\left(\cos w\left(t-\frac{z}{V_p}\right) - \cos wt\right)\right] \end{aligned}\right\} \tag{15}$$

Equations (12) and (15) for the seismic active case of earth pressure match exactly with those obtained by Choudhury and Nimbalkar, 2006 for a specific case of f = 1.0, and that of Steedman and Zeng, 1990 for a specific case of $k_v = 0$.

The acting point of P_{ad}, H_d above the base can be found by taking moments about the base of the wall. Then, if M_d is the dynamic component of the bending moment

$$H_d = \frac{M_d(z=H)}{P_{ad}\cos\delta} = \int_0^H \frac{p_{ad}\cos\delta(H-z)dz}{P_{ad}\cos\delta} \tag{16}$$

where, m = $\lambda\, k_h \cos(\alpha-\phi)$ and n = $\eta\, k_v \sin(\alpha-\phi)$. Thus, H_d is the function of H/TV_s, H/TV_p, f and t.

RESULTS AND DISCUSSIONS

In the case of cohesionless soils, to avoid the phenomenon of shear fluidization (i.e. the plastic flow of the material at a finite effective stress) for the certain combinations of k_h and k_v (Richards et al., 1990) the values of ϕ considered in the analysis are to satisfy the relationship given by,

$$\phi > \tan^{-1}\left[\frac{k_h}{1-k_v}\right] \tag{17}$$

Results are presented in the tabular and graphical form for normalized seismic active earth pressure along the normalized depth of the wall. Variation of parameters considered is as follows:
$\phi = 20^0, 30^0, 35^0$ and 40^0
$\delta = -0.5\phi$, 0,0.5ϕ and ϕ.
k_h = 0.0, 0.1, 0.2, 0.3.
$k_v = 0.0k_h$, $0.5k_h$ and k_h.
f = 1.0, 1.2, 1.4, 1.6, 1.8 and 2.0

Seismic active earth pressure coefficient (K_{ae})

Figure 2 shows the effect of soil amplification on the seismic active earth pressure coefficient (K_{ae}) for different values of k_h with $k_v = 0.5k_h$, $\phi = 35^0$, $\delta = \phi/2$, $H/TV_s = 0.3$, $H/TV_p = 0.16$. From the plot, it may be seen that the seismic active earth pressure coefficient (K_{ae}) increases with increase in soil amplification factor and the rate of increase is more for higher values of k_h. For example, when k_h

= 0.3, seismic active earth pressure coefficient, K_{ae} increases by, 20.1% when f_a changes from 1.0 to 1.2, 16.72% when f_a changes from 1.2 to 1.4, 14.32% when f_a changes from 1.4 to 1.6, 12.53% when f_a changes from 1.6 to 1.8, and 11.13% when f_a changes from 1.8 to 2.0. Thus, the present study reveals the significant influence of soil amplification on the seismic active earth pressure coefficient.

Normalised seismic active earth pressure distribution

Figure 3 shows the effect of soil amplification on normalized distribution of the seismic active earth pressure with $k_h = 0.3$, $k_v = 0.15$, $\phi = 35^0$, $\delta = \phi/2$, $H/TV_s = 0.3$, $H/TV_p = 0.16$. Seismic active earth pressure shows marginal increase near the top of the retaining wall and relatively more increase at the bottom of the wall with the increase in soil amplification factor, f_a. At the bottom of the retaining wall, the seismic active earth pressure increases by about 5.79 % when f_a changes from 1.0 to 1.2, 5.47 % when f_a changes from 1.2 to 1.4, 5.18 % when f_a changes from 1.4 to 1.6, 4.93 % when f_a changes from 1.6 to 1.8, and 4.7 % when f_a changes from 1.8 to 2.0. While at the mid-height of the wall, seismic active earth pressure increases by about 6.43 % when f_a changes from 1.0 to 1.2, 6.04 % when f_a changes from 1.2 to 1.4, 5.7 % when f_a changes from 1.4 to 1.6, 5.4 % when f_a changes from 1.6 to 1.8, and 5.1 % when f_a changes from 1.8 to 2.0. It also shows the non-linear distribution of the seismic active earth pressure under different soil amplification factors.

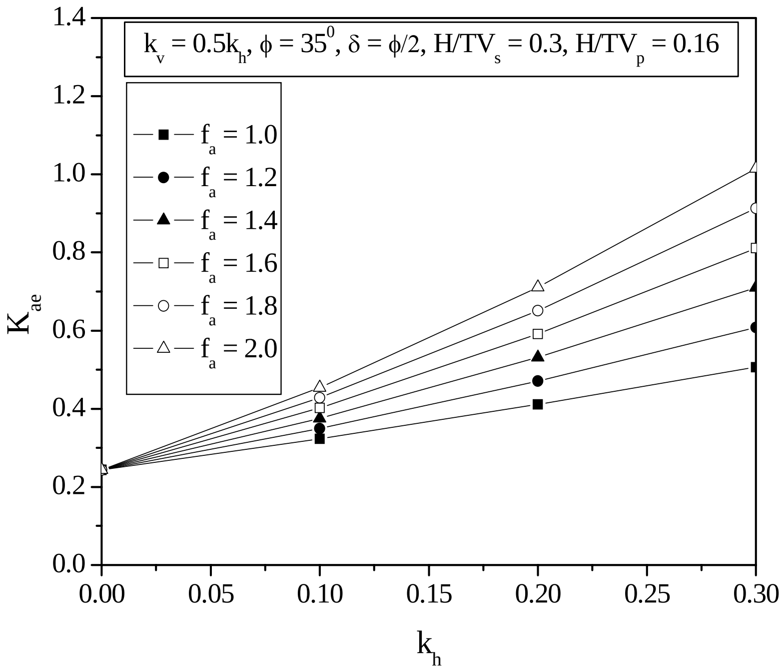

Figure 2. Effect of soil amplification on seismic active earth pressure coefficient (K_{ae}) for different values of k_h with $k_v = 0.5k_h$, $\phi = 30^0$, $\delta = \phi/2$, H/TVs = 0.3, $H/TV_p = 0.16$.

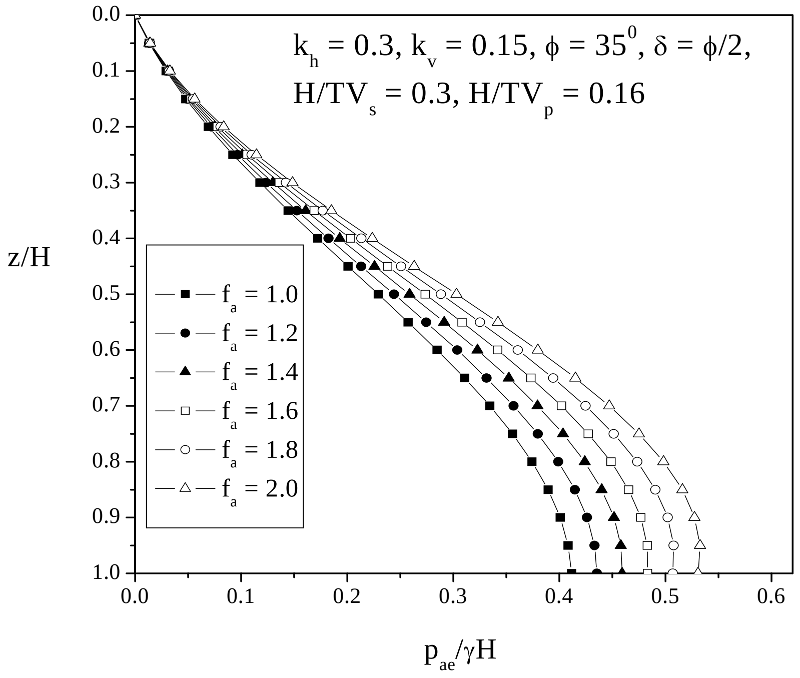

Figure 3. Effect of soil amplification on normalized seismic active earth pressure distribution with $k_h = 0.3$, $k_v = 0.15$, $\phi = 30^0$, $\delta = \phi/2$, $H/TV_s = 0.3$, $H/TV_p = 0.16$.

Point of location of dynamic thrust increment (H_d)

The values of point of location of dynamic active thrust increment (H_d) are given in Table 1 for different values of k_h, k_v, δ and ϕ. It is evident from Table 1 that, the magnitudes of the point of location of dynamic active thrust increment (H_d) increases with the increase in both the horizontal and vertical seismic accelerations. For example, when k_h changes from 0.0 to 0.2, for the case of $\delta = 0^0$, $\phi = 30^0$ and $k_v = 0.0$, the value of H_d is increased by 20.7 %. Again for the case of $\delta = 15^0$, $\phi = 30^0$ and $k_v = 0.5k_h$, the value of H_d is increased by 25.8 %.

Table 1. Point of location of dynamic active thrust increment (H_d) for different values of k_h, k_v, , δ and ϕ with $H/\lambda = 0.3$, $H/\eta = 0.16$, f = 1.2

		k_h											
ϕ	δ	0.0	0.1			0.2			0.3		
		k_v	k_v			k_v			k_v		
		0.0	0.0	0.05	0.1	0.0	0.1	0.2	0.0	0.15	0.3
20	-10	0.333	0.403	0.419	0.431	0.433	0.460	0.475	-	-	-
	0	0.333	0.397	0.412	0.422	0.441	0.456	0.473	-	-	-
	10	0.333	0.395	0.409	0.422	0.446	0.462	0.473	-	-	-
	20	0.333	0.398	0.412	0.420	0.454	0.464	0.473	-	-	-
30	-15	0.333	0.383	0.399	0.407	0.412	0.433	0.452	0.449	0.471	-
	0	0.333	0.369	0.384	0.391	0.402	0.420	0.436	0.447	0.460	-
	15	0.333	0.361	0.369	0.384	0.403	0.419	0.426	0.454	0.456	-
	30	0.333	0.364	0.376	0.384	0.413	0.423	0.433	0.474	0.470	-
40	-20	0.333	0.343	0.359	0.368	0.377	0.396	0.412	0.412	0.431	0.450
	0	0.333	0.308	0.325	0.330	0.353	0.363	0.377	0.384	0.399	0.411
	20	0.333	0.296	0.311	0.317	0.337	0.351	0.365	0.386	0.388	0.405
	40	0.333	0.319	0.325	0.331	0.367	0.373	0.381	0.421	0.416	-

(- indicates that results are not available due to nonconvergence of the solution)

COMPARISON OF RESULTS

Table 2 shows the comparison of the results of point of application of the total seismic active/passive thrust with the already published research (Mononobe-Okabe, 1926, 1929, Steedman and Zeng, 1990, Richards and Elms, 1979) and the current available design recommendations in codes (IS 1893 – 1984, Eurocode 8 – 1998). From Table 2, it is clear that the results of point of application of the total seismic active/passive thrust, computed by the pseudo-dynamic method compare well with that obtained by Steedman and Zeng, 1990 for the active case due to similarity of the method and the difference is attributed to the consideration of the vertical seismic acceleration in the present study. However, the other values are obtained by using pseudo-static method with different theories which considers only linear distribution of the seismic earth pressure. Hence the present solution gives a logical formulation of the problem and presentation of the result which is required for the design purpose.

Table 2. Comparison of point of application of total active thrust obtained by the present study with available methods for H = 10 m, $\phi = 34^0$, $\delta = 17^0$, $\gamma = 17.3$ kN/m^3, $k_h = 0.3$, $k_v = 0.3$, f = 1.0

Methods	Point of application of total active thrust (h)
Mononobe-Okabe (1926,1929)	0.453H
Steedman and Zeng (1990)	0.384H
Richards and Elms (1979)	0.388H
IS 1893 (1984)	0.453H
Eurocode 8 (1998)	0.388H
Present study	0.409H

CONCLUSIONS

In the present analysis, pseudo-dynamic method which considers the time, phase change and amplification effect in body waves viz. shear and primary waves propagating through the backfill of the retaining wall, is applied to determine seismic active earth pressure coefficients, earth pressure distribution and the point of location of seismic active thrust. Effect of various parameters such as wall friction angle (δ), soil friction angle (ϕ), shear wave velocity (V_s), primary wave velocity (V_p), both the horizontal and vertical seismic accelerations ($k_h g$ and $k_v g$) and amplification factor (f) on seismic earth pressures behind rigid retaining wall has been studied. Non-linearity of the seismic earth pressure distribution increases with seismicity, which leads to the shifting of the point of application of total active/passive thrust required for the design purpose. But the conventional pseudo-static approach gives only linear earth pressure distribution irrespective of static and seismic condition leading to a fixed point of application i.e. 1/3rd from the base of the wall, which is a major drawback in the analysis. Again, comparison of point of application of total active thrust is done with available methods in the literature.

REFERENCES

Choudhury, D., Nimbalkar, SS. and Mandal, JN. "Influence of soil-wall interface friction on pseudo-dynamic earth pressure", *Proc. of 8th U.S. National Conference on Earthquake Engineering (8NCEE)*, April 18-22, 2006, San Francisco, CA, USA.

Choudhury, D. and Nimbalkar, SS. "Pseudo-dynamic approach of seismic active earth pressure behind retaining wall", *Geotechnical and Geological Engineering*, Springer, The Netherlands, Vol. 24, No. 5, 1103-1113, 2006.

Choudhury, D. and Singh, S., "New approach for determination of static and seismic active earth pressure", *Geotechnical and Geological Engineering*, Springer, The Netherlands, Vol. 24, No. 1, 117-127, 2006.

Choudhury, D., Sitharam, TG and Subba Rao, KS. "Seismic design of earth retaining structures and foundations", *Current Science,* India, Vol. 87, No. 10, 1417-1425, 2004

Eurocode 8. "Design provisions for earthquake resistance of structures", 1998.

Green, RA, and Ebeling, RM. "Seismic analysis of cantilever retaining walls", *US Army Technical Report*, ERDC/ITL-TR-02-3, 2002.

Green, RA and Ebeling, RM. "Modeling the dynamic response of cantilever earth-retaining walls using FLAC", *Proceeding of the 3rd International Symposium on FLAC and FLAC3D: Numerical Modeling in Geomechanics*, October 2003, Sudbury, ON, Canada, 1-10. 2003.

Green, RA, Olgun, CG, Ebeling, RM and Cameron, WI., "Seismically induced lateral earth pressures on a cantilever retaining wall", *Earthquake Engineering*, ASCE, 133, 946-955, 2003.

IS 1893. *Indian Standard Criteria for Earthquake Resistant Design of Structures*, Part V fourth revision, 1984.

Kramer, SL. *Geotechnical Earthquake Engineering*, New Jersey, Prentice Hall, 1996.

Richards, R. Jr., and Elms, DG. ''Seismic behavior of gravity retaining walls.'' *J. Geotech. Engrg.*, ASCE, Vol. 105(4), 449–469, 1979.

Richards, R., Jr., Elms, DG. and Badhu, M., ''Dynamic fluidization of soils.'' *J. Geotech. and Geoenvir. Engrg.*, ASCE, Vol. 116(5), 740-759, 1990.

Richards, R. Jr., Hunag, C., and Fishman, KL. "Seismic earth pressure on retaining structures." *J. Geotech. And Geoenvir. Engrg.*, ASCE, Vol. 125(9), 771–778, 1999.

Saran, S. and Gupta, RP. "Seismic earth pressures behind retaining walls." *Indian Geotechnical Journal*, Vol. 33, No. 3, 195-213, 2003.

Steedman, RS. and Zeng, X. "The influence of phase on the calculation of pseudo-static earth pressure on a retaining wall", *Geotechnique,* Vol. 40, No. 1, 103-112, 1990.

Steedman, RS. and Zeng, X. "Centrifuge modeling of the effects of earthquakes on free cantilever walls", *Centrifuge, 91,* Balkema, Rotterdam, The Netherlands, 425– 430, 1991.